

# Lateral and Longitudinal Controllers in Vehicles

Dikshita Kothari  
SID: 500539170  
April 3, 2022

## I. INTRODUCTION

Introduced in the early 1980s, autonomous cars have had a revolutionary impact on the automobile industry. Statistically, driver error is a major factor in 94% of road accidents. [1] Higher levels of autonomy have the potential to reduce risky driver behaviors. It can reduce the devastation caused due to impaired driving, drugged driving, unbelted vehicle occupants, speeding and distraction. Therefore, automatic vehicles are safer, more reliable, user friendly and environment friendly.

This paper focuses on designing the longitudinal and lateral control system for a car. These controllers can be used to achieve safe, efficient and stable cruise control and lane change of autonomous vehicles. The objective of the design report is to obtain optimized controllers which minimize travel time, maintain safe distance between vehicles, satisfy the constraints of the chosen vehicle and comply with traffic rules and regulations.

TABLE 1. VEHICLE SPECIFICATIONS [2]

Model	MG Hector
Mass (m)	1600 kg
Area (A)	3.23 m <sup>2</sup>
Drag Coefficient (C <sub>D</sub> )	0.4
Wheelbase (l <sub>r</sub> + l <sub>f</sub> )	2.75 m

## II. LONGITUDINAL CONTROLLER (CRUISE CONTROL)

### A. Linearization

The non-linear system is given by,

$$m\dot{v} + \frac{1}{2}A\rho C_D v^2 = u$$

For this report we have taken  $\rho$  as 1.225 kg/m<sup>3</sup>.

Let  $k = \frac{1}{2} \frac{A\rho C_D}{m}$ . For the chosen car,  $k = 5 \times 10^{-4}$ .

Then the non-linear system becomes,

$$\dot{v} = \frac{u}{m} - kv^2 = f(v, u)$$

We select  $v_e, u_e$  as equilibrium points such that  $f(v_e, u_e) = 0$ .

If  $\delta_u = u - u_e$  and  $\delta_v = v - v_e$  are the deviations from the equilibrium, then the linear differential equation given below is a local and linear approximation to the non-linear dynamics.

$$\dot{v} = \frac{(u - u_e)}{m} - 2kv_e(v - v_e)$$

Three equilibrium points are chosen, and the corresponding linearized equations are given below.

TABLE 2. EQUILIBRIUM POINTS AND LINEARIZED EQUATIONS

No.	$v_e$	$u_e$	Linearized Equation
1	0	0	$\dot{v} = \frac{u}{m}$
2	$1/\sqrt{k}$	m	$\dot{v} = \frac{u}{m} - 2\sqrt{k}v + 1$
3	$1/\sqrt{2k}$	2m	$\dot{v} = \frac{u}{m} - 2\sqrt{2k}v + 2$

The initial condition selected is  $v(0) = 15\text{m/s}$  (speeding). As the vehicle is moving at uniform velocity, the acceleration  $\dot{v} = 0$ . The corresponding force demanded by the engine is,

$$u = \frac{1}{2}A\rho C_D v^2 = 180\text{ N}$$

The linearized equations were plotted on Simulink and the results obtained are given below.

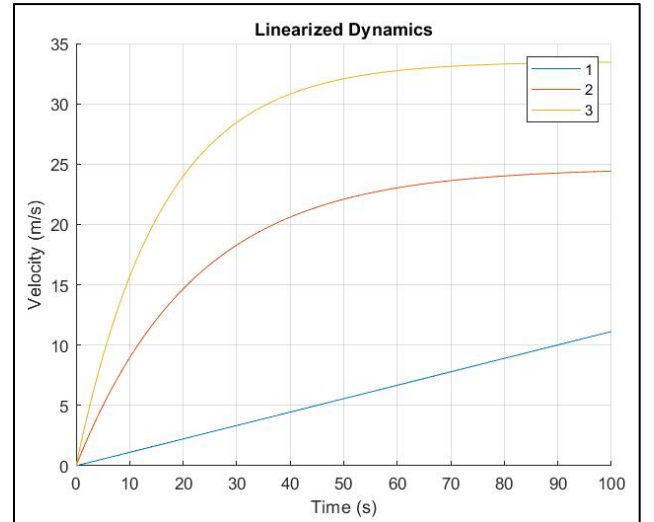


Fig. 1. Linearized System Dynamics.

The graphs plotted above are the open loop transient response of the system. It can be concluded that the first linear equation does not stabilise like the other two. The physical interpretation is that the velocity keeps on increasing at constant force and at constant acceleration. Although this system can be stabilized using feedback mechanisms, it will be difficult to control. Therefore, it is not used for further analysis.

The second and third plots obtained are analogous to each other and stabilize at different velocities. The velocity at which the latter stabilizes is  $\sqrt{2}$  times the former. This is as expected because the equilibrium point for velocity chosen for the latter is  $\sqrt{2}$  times the former. The system accelerates until

a particular velocity after which the acceleration becomes zero and the vehicle moves at a constant velocity. These are desirable results as the system is stable and can be controlled easily.

### B. PID Controller Design

A Proportional-Integral-Derivative (PID) controller is used as it employs a feedback mechanism to continuously monitor the speed of the vehicle and ensure that it traverses at the reference value despite present disturbances. It makes the system robust and is easy to implement using filters. The integral component of the controller helps to mitigate steady state error ensuring that the chosen cruise control speed is maintained. The derivative component of the controller helps to stabilise the system and speeds up the transient response ensuring that the vehicle reaches cruise control speed quickly.

The equilibrium point fixed for control is  $v_e = 1/\sqrt{k}$  and  $u_e = m$ . The linearized equation is,

$$m\dot{v} + 2m\sqrt{k}v - m = u$$

The forced input (u) to the system is taken as,

$$u = K_P(r - v) + K_D(\dot{r} - \dot{v}) + K_I \int (r - v) d\tau$$

Both these equations are differentiated and the derivative of the forced input ( $\dot{u}$ ) is eliminated.

$$m\ddot{v} + 2m\sqrt{k}\dot{v} = K_P(\dot{r} - \dot{v}) + K_D(\ddot{r} - \ddot{v}) + K_I(r - v)$$

Substituting  $r = e^{st}$  and  $v = G(s)e^{st}$  we get the transfer function of the controlled system G(s) as,

$$G(s) = \frac{\frac{K_D s^2 + K_P s + K_I}{m + K_D}}{s^2 + \frac{2m\sqrt{k} + K_P}{m + K_D}s + \frac{K_I}{m + K_D}}$$

TABLE 3. TIME DOMAIN SPECIFICATIONS

Reference Speed (r)	11 m/s or 40 km/h
Settling Time ( $t_s$ )	8 s
Rise Time ( $t_r$ )	2.8 s
Peak Overshoot ( $M_p$ )	2 %
Damping Ratio ( $\zeta$ )	0.78
Natural Frequency ( $\omega_n$ )	0.64

Comparing the obtained transfer function to the generalized transfer function of a second order system, we get the following values for the feedback gains in the controller.

TABLE 4. CONTROLLER GAINS

Proportional ( $K_P$ )	2000
Integral ( $K_I$ )	850
Derivative ( $K_D$ )	470

The linearized system transfer function is given by,

$$G(s) = \frac{1}{ms + 2m\sqrt{k}}$$

The PID controller is given by  $K(s) = K_P + K_D s + \frac{K_I}{s}$ .

The transient response of the controlled linearized system is as expected. The response is underdamped ( $\zeta < 1$ ) and has the decided time domain specifications.

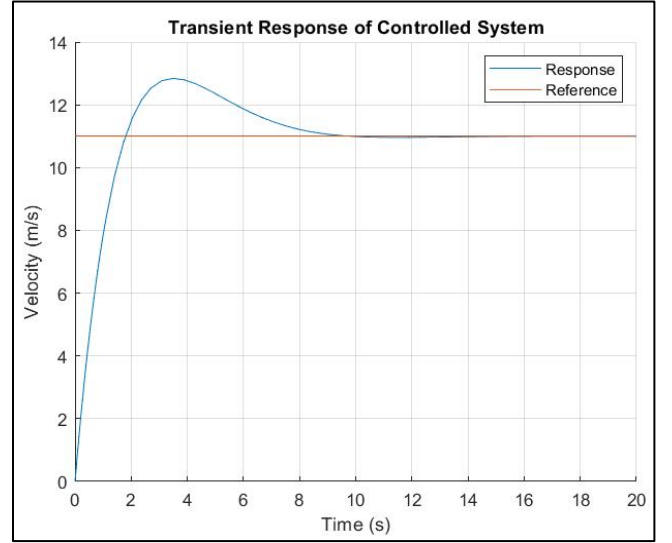


Fig. 2. PID Controlled System Response.

Settling time is the time taken by the system to reach 98% of steady state value. The rise time is the time taken by the system to go from 10% to 90% of the final value. The peak overshoot is the percentage difference between the maximum amplitude and stable value. It can be confirmed that these values are comparable to the design parameters.

### NUMERICAL EXPERIMENTS ON THE LINEAR MODEL

#### Varying Cruise Control Velocity

The vehicle may need to change speeds to adhere to traffic norms, as a result the reference speed may keep changing. The speed limit for school zones is 20 km/h, for normal city roads is 60 km/h and for the highway 100 km/h.

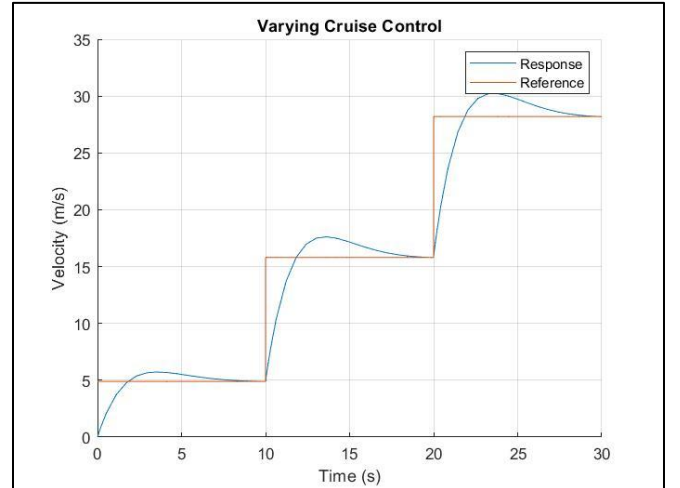


Fig. 3. Controller performance for varying reference velocities.

The controller is performing efficiently at different cruise control velocities and is even suitable for changing the cruise control velocity.

#### Varying Mass

The mass of the car may change dependent on the amount of fuel and the number of passengers. A range of masses are tested from 1500 kg to 1700 kg. It is observed that the controller performs efficiently for all masses in the range. Higher mass implies smaller overshoot and smaller settling

time. The reference velocity has been lowered for this analysis.

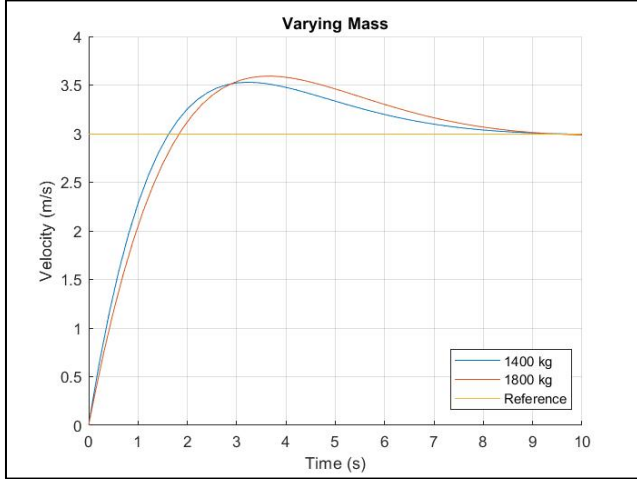


Fig. 4. Controller performance for varying mass.

#### Varying Air Density

It is known that the density of air decreases with increase in altitude or temperature. A range of air densities are tested from 0.3 to 3 kg/m<sup>3</sup>. The reference velocity has been lowered for this analysis. No change is observed.

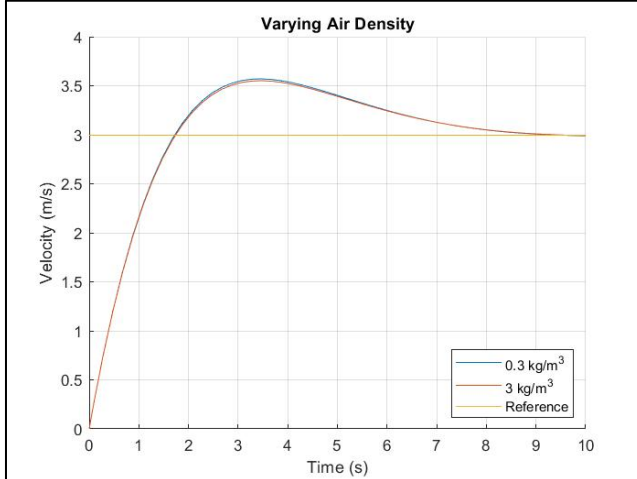


Fig. 5. Controller performance for varying air density.

#### Varying Drag Coefficient

The drag coefficient depends on several factors including the wind velocity, location of the car (in the wake of a large vehicle) and condition of the car (windows rolled down). The reference velocity has been lowered for this analysis.

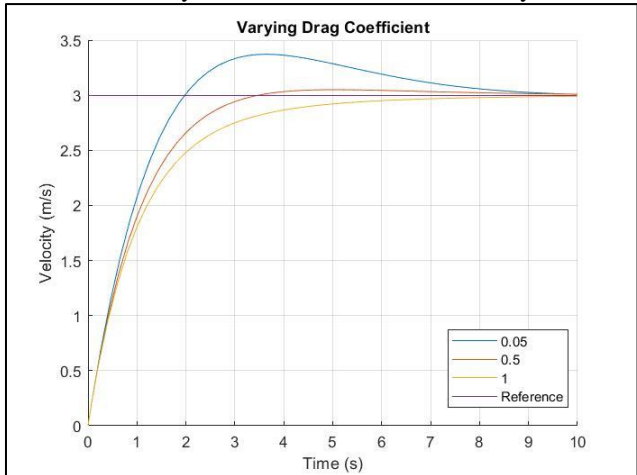


Fig. 6. Controller performance for varying drag coefficient.

It is observed that peak overshoot is inversely proportional to drag coefficient.

#### Testing on SUVs

The system parameters  $k$  and  $m$  were varied to view the performance of the controller on other SUVs.

TABLE 5. SUV SPECIFICATIONS

Model	Mass (kg)	Area (m <sup>2</sup> )	Parameter $k$ ( $\times 10^{-4} \text{ m}^{-1}$ )
Audi Q8 [3]	2300	3.4	3.62
Honda HR-V [4]	1300	2.864	5.4
Cadillac Escalade [5]	2556	4	3.83

The results are graphed below.

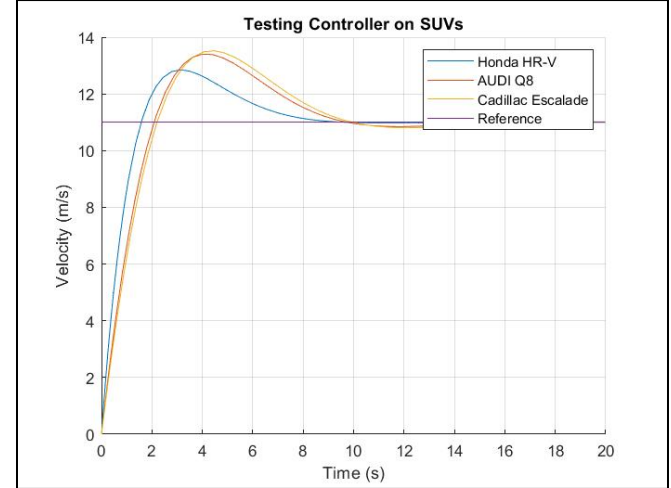


Fig. 7. Numerical Experiments on linear model

It is observed that vehicles having higher mass (Audi and Cadillac) have rise time, settling time and peak overshoot greater than specified. This is due to the derived transfer function  $G(s)$ , higher mass increases the natural frequency and decreases the damping ratio. Similarly, vehicles of lower mass (Honda) have a lower natural frequency and higher damping ratio, decreasing the rise time, settling time and peak overshoot. Therefore, the control system is effective and efficient and can be used for a variety of vehicles with similar mass and frontal area.

#### C. Validation

To validate the controller, we must test it against some real-world conditions. When implementing the control signal in the actuator there may be some external disturbances like a slope. Here we consider a slope of 15% grade which suggests an angle of inclination of  $\theta = 8.53^\circ$ . The effect of friction is ignored.

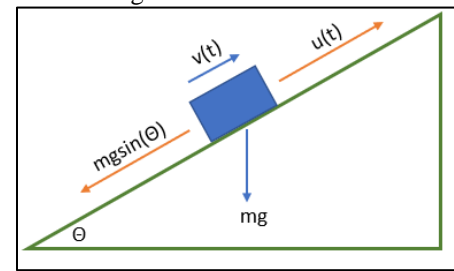


Fig. 8. Free Body Diagram of vehicle on a slope.

The real input affecting the system is  $u(t) + d$ . Plugging that into the non-linearized system we obtain the equation,

$$m\dot{v} + \frac{1}{2}A\rho C_D v^2 = u - mg\sin(\theta)$$

The disturbance is added at 20 seconds. Substituting the linear controller for reference tracking into this system we get the following desirable response.

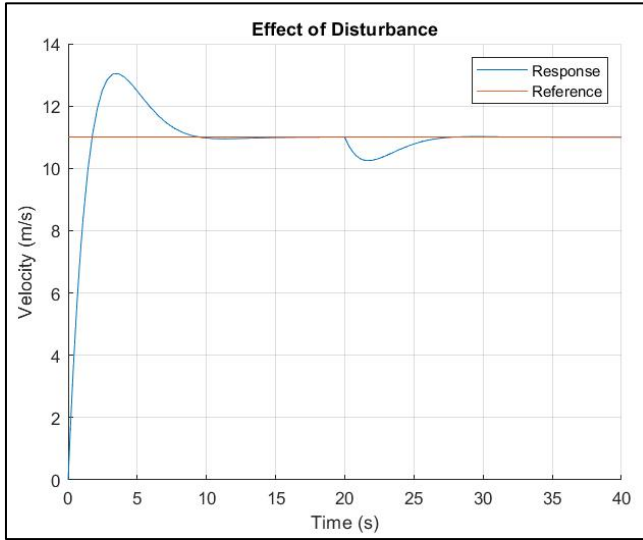


Fig. 9. Variation in velocity with time due to slope.

The physical interpretation of the undershoot observed at 20 seconds is that the vehicle slows down initially as it encounters the slope but the PID cruise controller efficiently monitors and adjusts the speed of the vehicle. The undershoot observed is due to the addition of a positive zero to the system.

The controller is tested for different cruise control (reference) velocities.

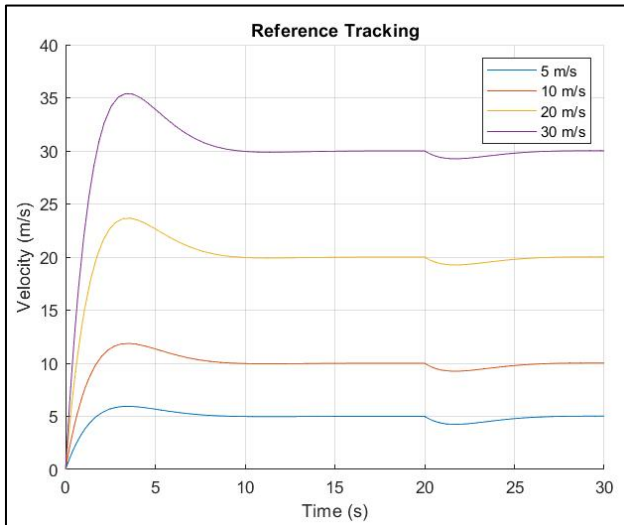


Fig.10. Closed loop dynamics for different reference speeds.

The controller performance is desirable at all velocities. The response without disturbance is proportional to the reference and the undershoot due to disturbance is same for all reference velocities. The controller is stable, effective and efficient at all velocities.

#### Effect of feedback gains on system response characteristics

To further validate the system, the system response characteristics like overshoot, rise time, settling time and steady state error for varying feedback gains ( $K_P$ ,  $K_D$  and  $K_I$ ) is studied.

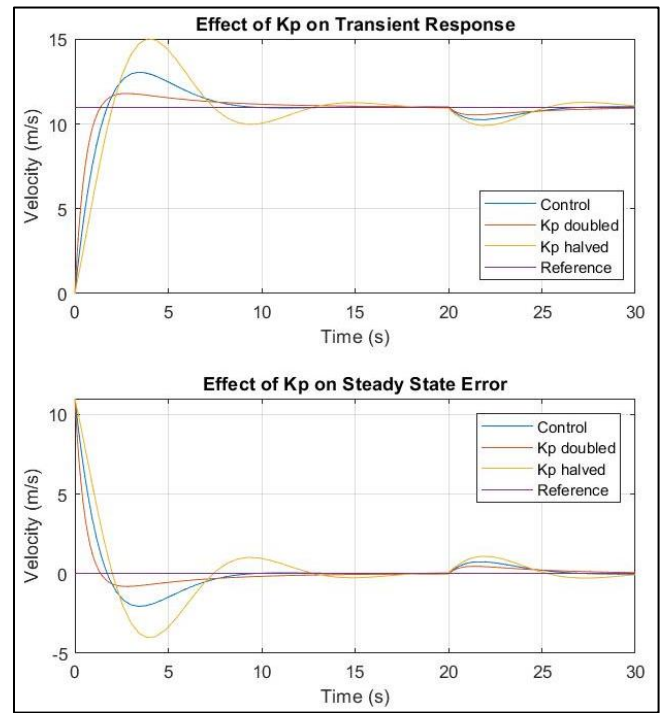


Fig. 11. Effect of proportional gain on system response characteristics.

$K_P$  is inversely proportional to the settling time and peak overshoot. Reducing  $K_P$  increases the number of oscillations about the reference. This implies that the steady state error decreases with an increase in  $K_P$ .

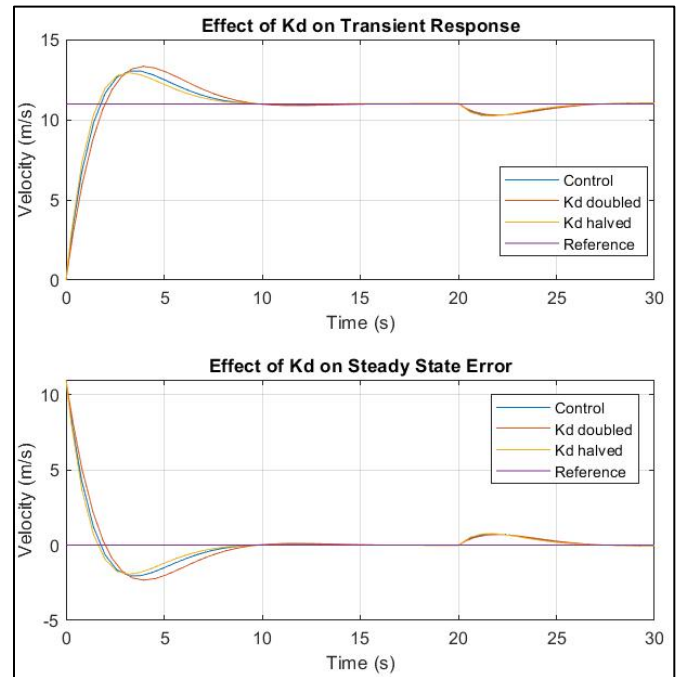


Fig. 12. Effect of derivative gain on system response characteristics.

$K_D$  is directly proportional to the peak overshoot, rise and settling time. Smaller values of  $K_D$  result in greater system stability. No change is observed in the steady state error of the system.

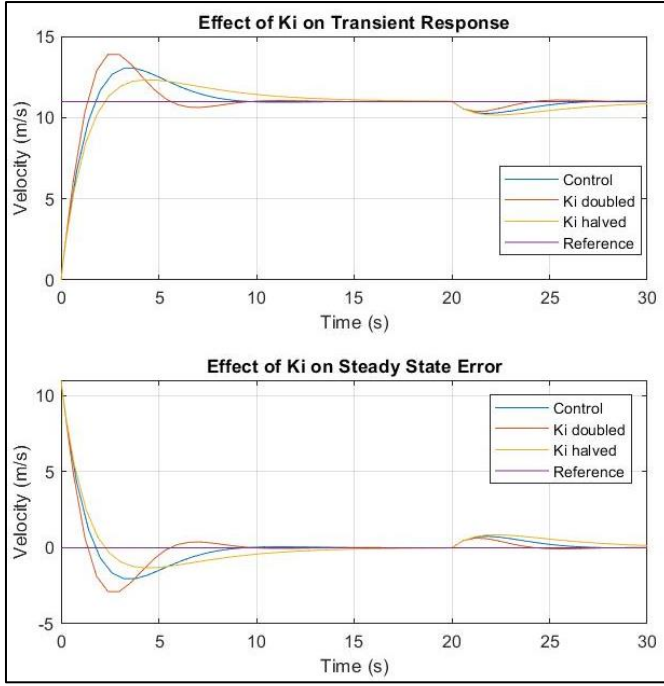


Fig. 13. Effect of integral gain on system response characteristics.  $K_I$  is directly proportional to the peak overshoot and settling time and inversely proportional to the rise time. Increasing the value of  $K_I$  eliminates steady state error from the system which is a desirable quality.

TABLE 6. EFFECT OF INCREASING FEEDBACK GAINS ON TRANSIENT RESPONSE

Gain	$\zeta$	$T_s$	$T_R$	$M_p$
$K_P$	Increases	Minor	Decreases	Decreases
$K_D$	Decreases	Increases	Minor	Increases
$K_I$	Decreases	Increases	Decreases	Increases

TABLE 7. EFFECT OF INCREASING FEEDBACK GAINS ON STEADY STATE ERROR AND STABILITY

Gain	Steady State error	Stability
$K_P$	Decreases	Decreases
$K_D$	No Change	Increases for small values
$K_I$	Eliminated	Decreases

### III. LATERAL CONTROL (LANE CHANGING)

In this section we need to design and test a controller for automatic lane changing. We assume that the vehicle is moving at some constant velocity implying that the acceleration is zero.

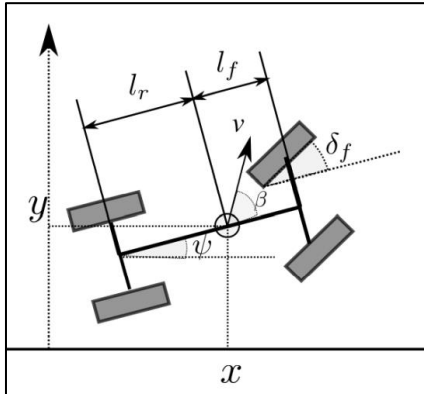


Fig. 14. Illustration of the vehicle parameters.

The steering wheel angle  $\delta_f$  is considered as the control input. The wheelbase for the selected car is 2.75 m.

#### A. Linearization

The motion of the center of mass (CoM) position of the car can be coupled to the longitudinal dynamics using the following equations. Small angle approximations are used to find a relation between the output (lateral position  $y$ ) and the control input (steering wheel angle  $\delta_f$ ).

$$\begin{aligned}\dot{x} &= v \cos(\Psi + B) = v \\ \dot{y} &= v \sin(\Psi + B) = v(\Psi + B) \\ \dot{\Psi} &= \frac{v}{l_r} \sin B = \frac{vB}{l_r}\end{aligned}$$

The relation between  $\delta_f$  and the CoM rotation angle  $B$  is given by,

$$\tan B = \frac{l_r}{l_r + l_f} \tan \delta_f$$

Approximating small angles and assuming  $l_r = l_f$  we get,

$$B = \delta_f / 2$$

Differentiating  $\dot{y} = v(\Psi + B)$  and substituting for  $\Psi$  and  $\dot{B} = \delta_f / 2$  we get,

$$\ddot{y} = \frac{v}{2} \delta_f + \frac{v^2}{2l_r} \delta_f$$

Which is a local and linear approximation for the system dynamics.

Substituting  $y = e^{st} G(s)$  and  $\delta_f = e^{st}$  we get,

$$G(s) = \frac{v/2 s + v^2/2l_r}{s^2}$$

The poles of the system are zero which makes the system marginally stable. This means that the output doesn't blow up or converge to equilibrium at some input value. We choose the speed  $v_0 = 5 \text{ m/s}$ . Comparing with the given equation we get,

$$A = \frac{v}{2} = 2.5 \text{ m/s}$$

$$B = \frac{v^2}{2l_r} = 9.1 \text{ m/s}^2$$

A and B are used as parameters for further control and analysis.

#### B. PD Controller Design

A Proportional Derivative controller is used to laterally control the car. A PD controller improves the stability of the system without affecting the steady state error. It improves the peak overshoot and reduces the rise and settling time increasing the speed of the transient response.

The distance between lanes (reference) is assumed to be 3.5 m. The equation of the controller is given by,

$$\delta_f = K_P(r - v) + K_D(\dot{r} - \dot{v})$$

Differentiating and substituting into the linearized dynamics,

$$\begin{aligned}\ddot{y} &= \frac{v}{2} [K_P(\dot{r} - \dot{v}) + K_D(\ddot{r} - \ddot{v})] \\ &\quad + \frac{v^2}{2l_r} [K_P(r - v) + K_D(\dot{r} - \dot{v})]\end{aligned}$$

Substituting  $r = e^{st}$  and  $v = G(s)e^{st}$  we get the transfer function of the controlled system  $G(s)$  as,



$$G(s) = \frac{AK_D s^2 + (AK_P + BK_D)s + BK_P}{s^2 + \frac{AK_P + BK_D}{1 + AK_D}s + \frac{BK_P}{1 + AK_D}}$$

The time domain specifications are chosen as below,

TABLE 8. TIME DOMAIN SPECIFICATIONS

Rise Time ( $t_r$ )	4 s
Settling Time ( $t_s$ )	8 s
Peak Overshoot ( $M_p$ )	5 %
Damping Ratio ( $\zeta$ )	0.7
Natural Frequency ( $\omega_n$ )	0.714

Comparing the obtained  $G(s)$  with standard transfer functions for second order systems we obtain the PD controller as,

$$K(s) = K_P + K_D s = 0.07337 + 0.1237s$$

For the chosen speed of 5 m/s, damping ratio ( $\zeta = 0.7$ ) is less than 1 which implies that the system is underdamped. It will overshoot 5% before approaches stability. The vehicle will have smooth and accurate transition from lane to lane.

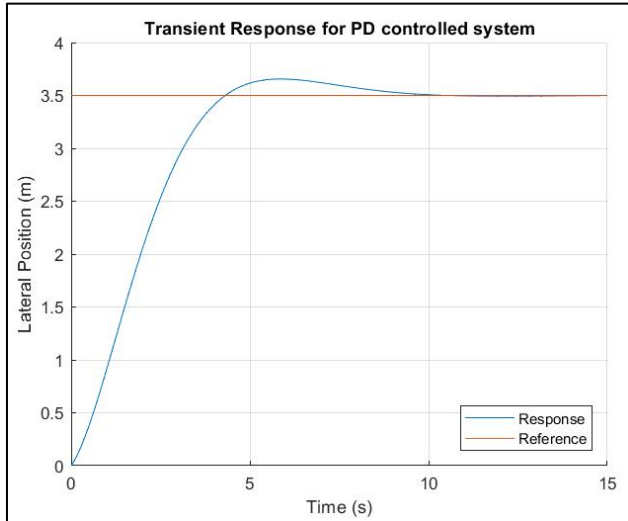


Fig. 15. Lane to lane transition.

The transient response is consistent with the specifications and the lane transition is smooth and accurate.

### C. Validation

To validate the controller, we must test it against some real-world conditions. The control signal may be implemented at any velocity and the controller must work efficiently in all those cases.

#### Lane Change Maneuver

The closed loop system response for the linear model is simulated and plotted for a variety of speeds. The parameters A and B are changed in the transfer function to accommodate the change in velocity.

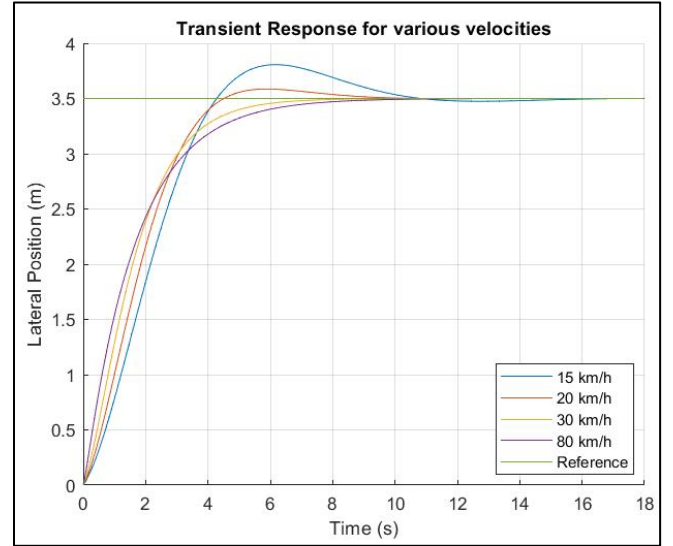


Fig. 16. Lane changing at different velocities.

Changing the velocity has a reasonable effect on the system. Damping is a reduction in the amplitude of an oscillation as a result of energy being drained from the system to overcome frictional or other resistive forces. The damping ratio is a dimensionless number describing the oscillations in a system. The damping ratio increases with the increase in velocity resulting in decrease in peak overshoot. There can be four types of damping in a system.

1. Underdamped ( $\zeta < 1$ ) – The system oscillates about the equilibrium point with reducing amplitude until it stabilizes. This is illustrated by the 15 km/h and 20 km/h plots.
2. Critically Damped ( $\zeta = 1$ ) – The system approaches stability as fast as possible with no oscillations. This is illustrated by the 30 km/h plot.
3. Overdamped ( $\zeta > 1$ ) – The system approaches stability with no oscillations. This is illustrated by the 80 km/h plot.
4. Undamped ( $\zeta = 0$ ) – The system oscillates about the equilibrium point without decay. This is highly undesirable for our system.

This indicates that at velocities higher than 30 km/h the system is always overdamped, and the vehicle will snap to the next lane without any oscillations resulting in a smoother and more accurate transition from one lane to the next. The controller is working efficiently for a large variety of velocities.

#### Reversing

The closed loop system response is simulated and plotted for negative speeds indicating that the system is reversing. The parameters A and B are changed in the transfer function to accommodate the change in velocity.

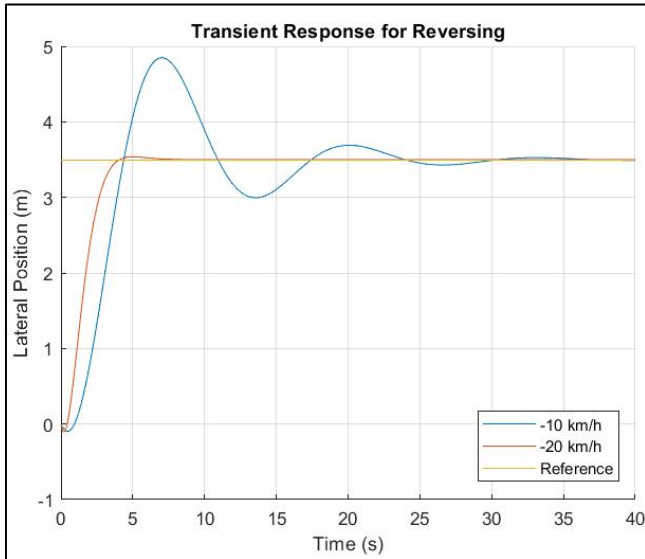


Fig. 17. Lane changing in reverse.

As discussed previously, the low magnitude velocity of 10 km/h has higher overshoot and larger settling time than 20 km/h due to the damping ratio.

TABLE 9. TIME DOMAIN SPECIFICATIONS (REVERSING)

Velocity	-10 km/h	-20 km/h
Damping Ratio ( $\zeta$ )	0.3	0.72
Natural Frequency ( $\omega_n$ )	0.5	1.8
Settling Time ( $t_s$ )	26.67 s	3 s
Rise Time ( $t_r$ )	3.6 s	1 s
Peak Overshoot ( $M_p$ )	37%	3.77%

When the vehicle is reversing, the initial velocity considered is negative resulting in the modified transfer function of the system to be,

$$G(s) = \frac{-v/2s + v^2/2l_r}{s^2}$$

Zeros are the values of  $s$  at which the numerator approaches zero value or the frequencies at which the response magnitude approaches zero value.

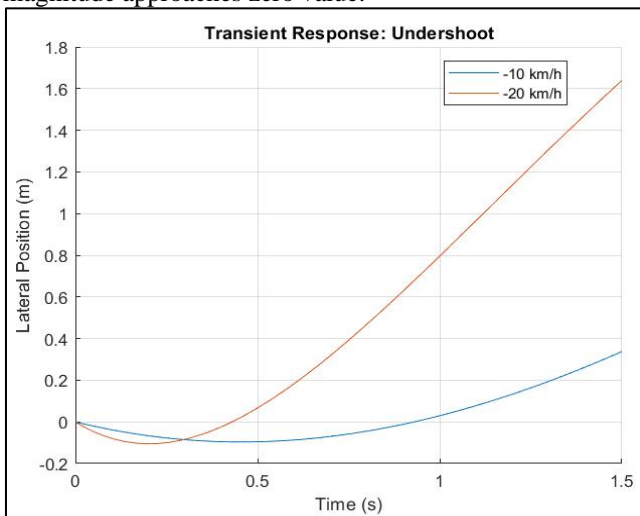


Fig. 18. Undershoot due to RHP zero.

This introduces a positive or right-hand plane zero into the system called nonminimum phase. Nonminimum phase systems are those which are causal and stable and whose inverses are causal and unstable. The negative zero has a larger contribution to the phase shift. Such systems will have maximum energy delay. A RHP zero makes the step response slower. It makes the system go in the opposite direction before going to equilibrium. Therefore, it is responsible for the undershoot observed in the graph.

The physical interpretation is that while reversing the vehicle traverses forward for a small amount of time before it reverses and changes the lane.

#### IV. CONCLUSION

This project designs and simulates cruise control and lane changing controllers. The detailed analysis of the cruise control system includes numerical experiments on the linearized model of the system, testing of the controller on different SUVs, reference tracking and effect of slope disturbance for the former and effect of changing velocity and reversing for the latter.

A PID controller is designed for the cruise control due to the small steady state error and fast response times. The effect of changing controller parameters on transient response is discussed in detail. The performance of the controller on a slope is tested to validate the system.

A PD controller is designed for the lane change due to the low overshoot and quick response times. The system is validated for different operating speeds and reversing speeds. Nonminimum phase systems and the effect of adding a right-hand plane zero is studied in detail.

The possible improvements on the design project are that the PID controller can be further tuned to follow the design specifications more closely. Additionally, some adjustments can be made to the lateral controller to reduce the negative effect of right-hand plane zeros on stability during reversing and eliminate undershoot. The controller can be designed using RLC networks ready to be used in vehicles.

#### REFERENCES

- [1] "Coalition for future mobility," [Online]. Available: <https://coalitionforfuturemobility.com/>.
- [2] "MG Hector Specifications," [Online]. Available: <https://www.mgmotor.co.in/vehicles/mghector/specifications>.
- [3] "AUDI Q8 Australian Specifications," August 2021. [Online]. Available: [https://www.audi.com.au/dam/nemo/australia/specification\\_guides/q8/Audi\\_Q8\\_Specification\\_Guide\\_MY22\\_010921.pdf](https://www.audi.com.au/dam/nemo/australia/specification_guides/q8/Audi_Q8_Specification_Guide_MY22_010921.pdf).
- [4] "Configurator: Build A Car," [Online]. Available: <https://www.honda.com.au/>.
- [5] "Cadillac Escalade/Escalade ESV - 2021," [Online]. Available: <https://media.cadillac.com/>.

## APPENDIX (SIMULINK)

### 1. Cruise Control

#### Linearization

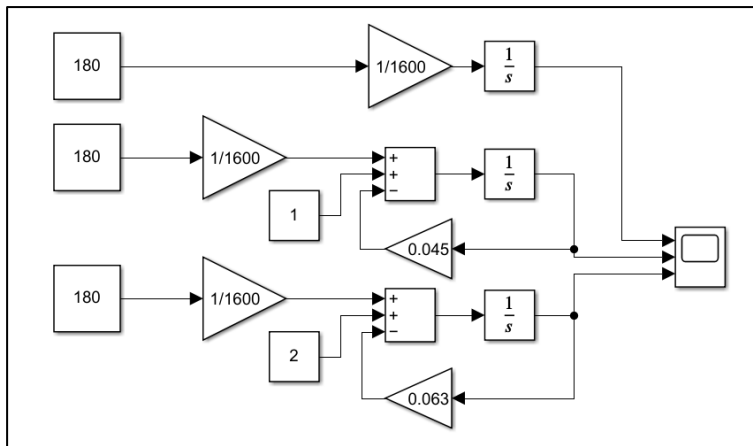


Fig. Linearized system

#### Controller Design (PID)

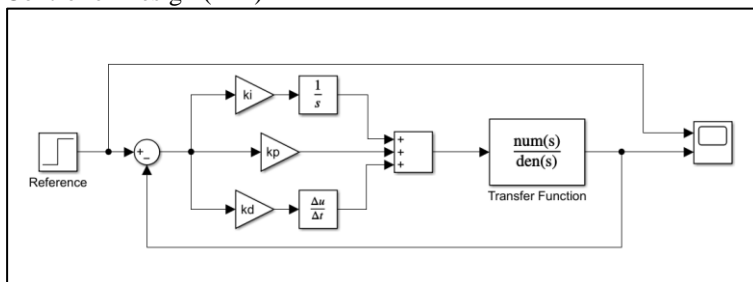


Fig. PID controlled system

#### Validation

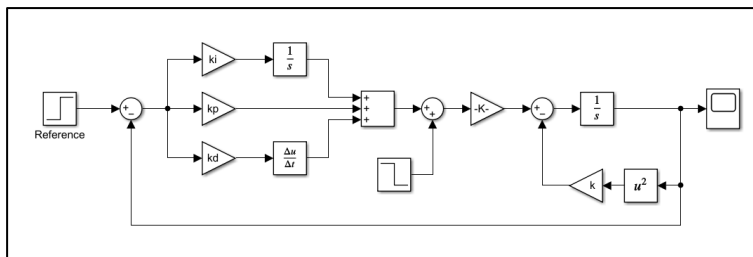


Fig. Addition of slope disturbance to non-linearized system

### 2. Lane Change

#### Controller Design (PD)

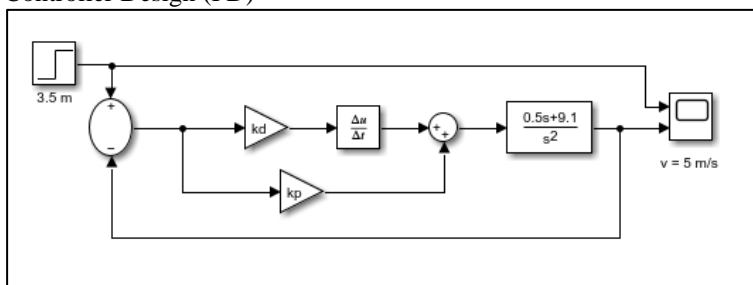


Fig. PD Controlled System